Acknowledgments

This research was supported in part by the Douglas Aircraft Company of the McDonnell Douglas Corporation under Contract AS-25260-C.

References

[1]Jameson, A., and Caughey, D. A., "Numerical Calculation of the Transonic Flow Past a Swept Wing," New York Univ. ERDA Rept. COO-3077-140, New York, June 1977.

[2]Yadlin, Y., and Caughey, D. A., "Diagonal Implicit Multigrid Solution of the Three-Dimensional Euler Equations," *Proceedings of the Eleventh International Conference on Numerical Methods for Fluid Dynamics*, Vol. 323, Lecture Notes in Physics, Springer-Verlag, Berlin, June 1988, pp. 597–601.

[3]Jameson, A., "Iterative Solution of Transonic Flows over Airfoils and Wings, Including Flows at Mach 1," *Communications on Pure and Applied Mathematics*, Vol. 27, 1974, pp. 283–309.

[4]Wang, L., and Caughey, D. A., "Numerical Calculation of the Transonic Potential Flow Past a Swept Wing—An Improved Version of Program Flo-22," Cornell Univ., Sibley School of Mechanical and Aerospace Engineering, Fluid Dynamics and Aerodynamics Rept. FDA 88-17, Ithaca, NY, Aug. 1988.

[5]Steckel, D. K., Dahlin, J. A., and Henne, P. A., "Results of Design Studies and Wind Tunnel Tests of High Aspect Ratio Supercritical Wings for an Energy Efficient Transport," NASA CR-159332, 1980.

Predicting Droplet Impingement on Yawed Wings

Michael B. Bragg*
University of Illinois at Urbana—Champaign, Urbana, Illinois 61821
and
Stanley H. Mohler Jr.†
Sverdrup Technology, Brook Park, Ohio 44142

Introduction

IN-FLIGHT, aircraft icing occurs when an aircraft encounters a cloud of small, supercooled water droplets. Therefore, the first step in any complete aircraft icing analysis must include impingement prediction of the water droplets on the critical aircraft surfaces. Traditionally wings have been analyzed using a strip-theory approach and two-dimensional methods. Experimental data on three-dimensional wings have not been available to validate these methods. However, with the recent development of three-dimensional droplet-impingement computational methods,[1–3] the capability now exists to evaluate the accuracy of two-dimensional methods applied to three-dimensional wings. In this technical note a procedure for using two-dimensional droplet-impingement techniques on three-dimensional wings is presented and evaluated against a full three-dimensional code for straight and yawed wings.

Received Feb. 22, 1991; revision received Oct. 15, 1991; accepted for publication Oct. 29, 1991.

*Associate Professor, Department of Aeronautical and Astronautical Engineering. Associate Fellow AIAA.

†Research Engineer, Combustion and Icing Section, LeRC Group. Member AIAA.

Numerical Procedure

Two-Dimensional

Here the Lagrangian, two-dimensional droplet-impingement code of Bragg[4] is used. The trajectory equation given below is a second-order, ordinary differential equation solved by a step-integration scheme:

$$K\left(\frac{d^2x}{d\tau^2}\right) = \frac{C_D R}{24}\left(V - \frac{dx}{d\tau}\right)$$

where K is defined in Table 1, R is the droplet Reynolds number, and C_D is the droplet-drag coefficient. V, x, and τ are the dimensionless local air velocity, droplet-position vector, and time, respectively. K and R_U are often combined[4] into a single dimensionless parameter K_0, the modified inertia parameter, that greatly reduced the analysis. K_0 is given by

$$K_0 = 18K[R_U^{2/3} - (\sqrt{6}/R_U)\arctan(R_U^{1/3}/\sqrt{6})]$$

Several single-droplet trajectories are computed from the freestream, far ahead of the airfoil, until they strike the airfoil. Using this information, a local nondimensional mass flux of droplet-impinging on the surface, referred to as the impingement efficiency, β, can be calculated.

The method for using a two-dimensional analysis to calculate the droplet impingement on a section of a swept or yawed finite wing is summarized in Table 1.

The two-dimensional analysis is performed on an airfoil section perpendicular to the leading-edge where only the component of the freestream velocity, $U_\infty \cos\Lambda$, is seen, therefore, R_U and K are calculated as shown. The two-dimensional analysis is performed at the section-lift coefficient seen by the appropriate section of the three-dimensional wing. In addition, the impingement efficiency β must be reduced by $\cos\Lambda$ since the two-dimensional section is exposed to only that portion of the freestream water droplet concentration.

Three-Dimensional

The three-dimensional droplet impingement code of Mohler[3] is used for comparison to the two-dimensional results. This code uses a three-dimensional surface panel method to generate the three-dimensional flowfield. To save computer time, flowfield velocities are stored at the nodes of a three-dimensional grid system and interpolated to obtain the velocities required by the differential equation solver. The trajectory equation, and the integration scheme, is basically the same as the two-dimensional case, but is done for all three directions x, y, and z. Whereas, the impingement efficiency is determined as a continuous function in the two-dimensional code; here an average value is determined over each panel of interest. The code iterates until a trajectory strikes a panel at each of the four corner points. Thus, the impingement efficiency is formed by the ratio of the effective particle streamtube cross-sectional area far in front of the body, to the surface panel area.

Table 1 Swept or yawed wing two-dimensional calculations

	3D	Equivalent 2D Values
R_U	$\frac{\rho\delta U_\infty}{\mu}$	$\left(\frac{\rho\delta U_\infty}{\mu}\right)\cos\Lambda$
K	$\frac{\sigma\delta^2 U_\infty}{18c\mu}$	$\left(\frac{\sigma\delta^2 U_\infty}{18c\mu}\right)\cos\Lambda$
β	β_{3D}	$\beta_{2D}\cos\Lambda$

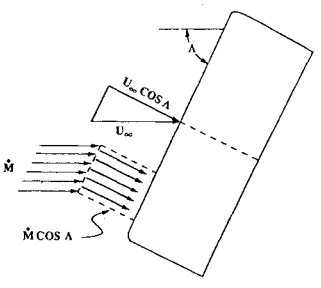

Results and Discussion

Four cases are compared to evaluate the accuracy of the two-dimensional model for three-dimensional wings. Figure 1 shows an aspect ratio 10, rectangular wing with a NACA 0012 airfoil section. Droplet impingement was calculated at the model centerline and 0.90 semispan location. The paneling in the three-dimensional code was concentrated in the impingement regions for the two cases to improve accuracy. Calculations were made at 0 and 30 deg of yaw. Note that the finite wing at 30-deg-yaw produced an asymmetric flowfield.

Figure 2 shows the two-dimensional and three-dimensional calculation on the model centerline with no yaw. Here, as in all comparisons, $R_U = 232.5$, $K = 0.2$ and the sectional-lift coefficient is 0.4 (Table 2). Note that the three-dimensional results can be identified by the regions of constant impingement efficiency, β, that is the average β on each surface panel. The two-dimensional results compare favorably to the three-dimensional results, although the total nondimensional mass flux/unit span (area under the curve) is somewhat different. The two-dimensional results yield 0.0309 while three-dimensional predicts 0.0324. This 5% error is somewhat larger than reported by Mohler[3] and is, in part, dependent upon the size and location of the surface panels.

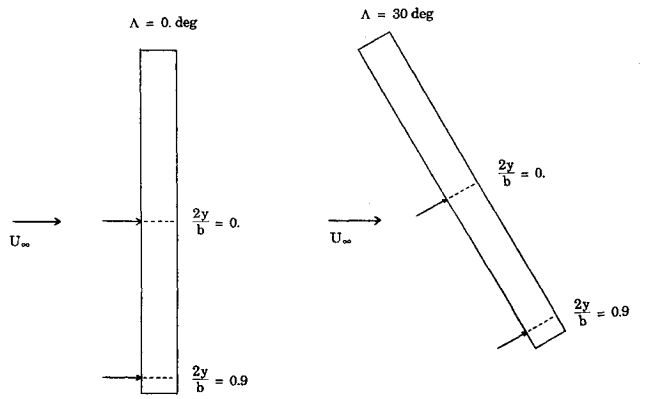

Fig. 1 Impingement locations on the aspect ratio 10 wing with and without yaw.

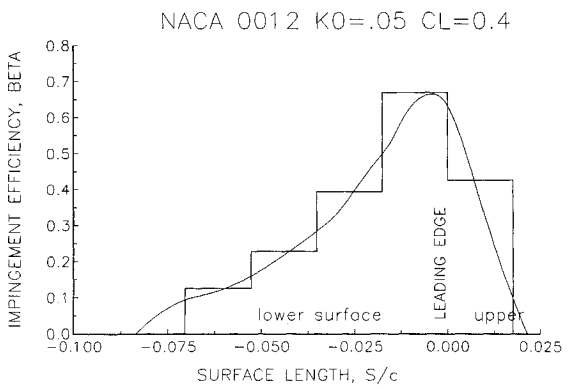

Fig. 2 Comparison of two-dimensional and three-dimensional calculations on the wing centerline with no yaw (continuous curve is the two-dimensional result).

The centerline impingement efficiency, with and without yaw are shown in Fig. 3. Note that the unswept values are the same as shown in Fig. 2. Here the effect of yaw is to reduce the droplet-impingement efficiency, particularly near the airfoil leading-edge, $S/c = 0$. The two-dimensional model predicts this reduction in β due to sweep reasonably well. While the total mass flux/unit span values, Δy_0, continue to be underpredicted, the two-dimensional models predict an 18% reduction in Δy_0 due to the yaw angle whereas the three-dimensional code gives a 13% reduction.

Of course, the real test of the two-dimensional method, is near the wing tip where the largest three-dimensional flowfield effects are seen. Figure 4 shows the two-dimensional and three-dimensional calculations near the wing tip, with, and without yaw. Note that the two-dimensional calculations are the same as shown in Fig. 3. Here the two-dimensional method fails to predict the effect of yaw in the three-dimensional results. With no yaw (dashed lines) the two-dimensional method predicts about 9% less mass than the three-dimensional code. However, with sweep, the three-dimensional code shows a large shift in the impingement efficiency to the lower surface with about the same total mass flux/unit span. The two-dimensional code predicts an overall decrease in total mass flux/unit span and no shift in distribution to the lower surface.

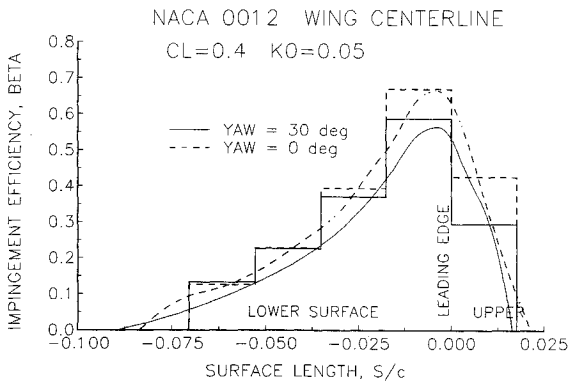

Fig. 3 Comparison of two-dimensional and three-dimensional calculation on the centerline with and without yaw (continuous curve is the two-dimensional result).

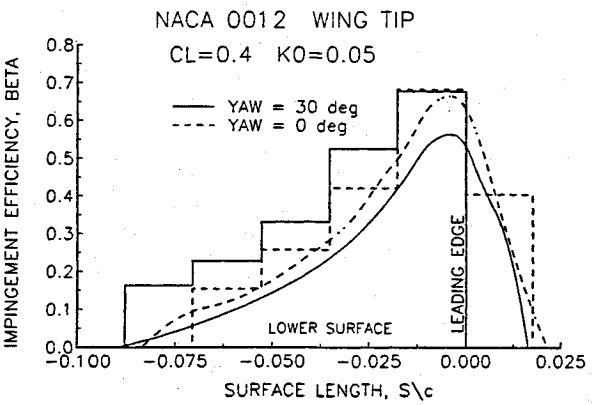

Fig. 4 Comparison of two-dimensional and three-dimensional calculation near the wing tip with and without yaw (continuous curve is the two-dimensional result).

Table 2 Data for the impingement results shown

Geometry	α, deg ($C_l = 0.4$)	R_U	K	K_0	$(2y/b)$	Λ, deg	Δy_0[a]
3D	4.26	232.5	0.2	0.05	0	0	0.0324
3D	5.69	232.5	0.2	0.05	0	30	0.0283
3D	6.66	232.5	0.2	0.05	0.9	0	0.0338
3D	13.20	232.5	0.2	0.05	0.9	30	0.0339
2D	3.31	232.5	0.2	0.05	—	0	0.0309
2D	3.31	201.4	0.173	0.046	—	30	0.0252

[a]Total nondimensional mass flux at a spanwise station/unit span.

The three-dimensional wing calculations are influenced by the increased wing circulation that results from the wing angle-of-attack, 13.2 deg, required to match the desired lift coefficient of 0.4 at the $2y/b = 0.9$ station.

Summary

On the model centerline where three-dimensional effects are small, the two-dimensional analysis presented, predicts reasonably well the droplet impingement on a three-dimensional yawed wing. Near the wing tip [$(2y/b) = 0.9$] the two-dimensional model fails to accurately predict the droplet-impingement on a yawed wing. Based on these calculations and the more detailed analysis of Ref. 3, it is clear that the two-dimensional analysis works well on yawed wings away from the tips. However, a three-dimensional analysis must be used near the tip of a finite wing. It is anticipated that in other cases where a significant three-dimensional flow field effect is present, a three-dimensional analysis would also be required.

Acknowledgment

This work was supported in part by B. F. Goodrich De-Icing Systems, Uniontown, Ohio.

References

[1]Norment, H. G., "Calculation of Water Drop Trajectories to and About Arbitrary Three-Dimensional Lifting and Nonlifting Bodies in Potential Airflow," NASA CR 3935, Oct. 1985.

[2]Kim, J. J., "Particle Trajectory Computation on a 3-D Engine Inlet," NASA CR 175023, Jan. 1986.

[3]Mohler, S. R., Jr., "A Three-Dimensional Droplet Trajectory Program for Aircraft Icing Analysis," M.S. Thesis, Ohio State Univ., Columbus, OH, 1990.

[4]Bragg, M. B., "Rime Ice Accretion and Its Effect on Aircraft Performance," NASA CR 165599, March 1982.

Demonstration of Structural Optimization Applied to Wind-Tunnel Model Design

Mark French* and Raymond M. Kolonay*
Wright Laboratory,
Wright-Patterson Air Force Base, Ohio 45433

Introduction

ONE of the most important tasks in the design of an aeroelastically scaled wind-tunnel model wing is making sure the stiffness characteristics are correct. The engineer must design a model structure whose stiffness characteristics match known values. These known values are derived by scaling the stiffness characteristics of the full-size structure that the model represents.

It is assumed that a target flexibility matrix is known for the scaled model. A column of a flexibility matrix represents the displacements at all the grid points on the wing due to a unit load at one grid point. If the desired flexibility matrix is known for the model, a displacement constraint can be written for the deflection at each grid point in the structure due to a unit load placed at some grid point. If a structure can be designed so that all the constraints are active; that is, they lie on the boundary of the feasible region, it will have the desired response to the unit load placed on it.

Using this approach, there is no need to know any more about the desired structure than the flexibility matrix and the basic geometry of the structure. The model's structure need not bear any resemblance to that of the original structure as long as the overall stiffness characteristics match the scaled stiffness of the full-size structure. The possibility then exists of modeling an anisotropic structure with an isotropic one.

Background

It has been shown that a general purpose structural optimization code can be used to simplify the wind-tunnel model design process considerably.[1,2] A general purpose finite-element-based analysis and optimization program[3] was used to design a structure made up of beam and plate elements. Using only the widths of the beam elements as design variables, a design was obtained that satisfied the stiffness constraints, and a sample structure was manufactured. The displacement of the structure due to loads applied at various grid points was measured using laser holographic techniques. The stiffness of the test article was found to agree well with the finite element predictions. The previous approach was more cumbersome than desirable because the program involved was applied to a problem for which it was not well suited. Also, the procedure resulted in a structure that was unnecessarily difficult to manufacture. To improve the design procedure, a new finite element based optimization program was written and the problem described in Ref. 1 was reworked using a different finite element representation.

Analysis

To allow easy comparison of the results between the current research and that cited in Ref. 1, the same 1/9-scale fighter wing was selected. The wing was constructed largely of composite materials and was built to demonstrate the feasibility of using aeroelastic tailoring on fighter wings (Fig. 1). The structure involved in this effort represents only the structural box of the original wing. Both the planforms of the previously manufactured test article[1] and model structure described here are the same size as the 1/9-scale wing.

Reference 4 presents a flexibility matrix generated from a finite element model of the 1/9-scale wing. Flexibility coefficients are given at 28 points on the surface of the wing. The location of these points is presented in Fig. 2. This flexibility matrix was used as the basis for the design of the test structure. A set of displacement constraints for the optimization problem can be written using a column of the flexibility matrix; a load is placed at some point on the wing and the terms from the column of the flexibility matrix are input as displacement constraints. Each column of the flexibility matrix is considered

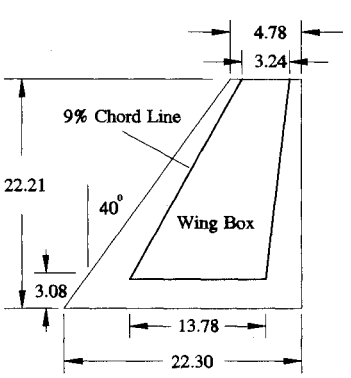

Fig. 1 Planform of 1/9-scale wing.

Received Feb. 20, 1991; revision received April 12, 1991; accepted for publication April 26, 1991. This paper is declared a work of the U.S. Government and is not subject to copyright protection in the United States.

*Aerospace Engineer. Member AIAA.